

## Supporting Information

### **Polymer grafting on nitrene functionalized green silica via “grafting from” and “grafting to” approach through enhanced spin capturing polymerization and 1,3-dipolar cycloaddition reaction**

Lukkumanul Hakkim N., Leena Nebhani\*

*Department of Materials Science and Engineering, Indian Institute of Technology Delhi, Hauz Khas, New Delhi 110016, India*

**Email: Leena.Nebhani@mse.iitd.ac.in**

#### **Sample abbreviations**

Table S1. Abbreviation of samples

S.No.	Sample description	Sample code
1	Control commercial precipitated silica	Control CPS
2	Mercaptopropyl functionalized commercial precipitated silica (Via post-modification)	MCPS
3	Nitrene-functionalized commercial precipitated silica	NCPS
4	Polystyrene grafted commercial precipitated silica via enhanced spin capturing polymerization (ESCP) of styrene	PS-CPS
5	Polystyrene grafted commercial precipitated silica via 1,3-dipolar cycloaddition of polystyrene macromonomer	PS-ene-CPS
6	Control commercial rice husk ash silica	Control CRHA
7	Mercaptopropyl functionalized commercial rice husk ash silica (via post-modification)	MCRHA
8	Nitrene-functionalized commercial rice husk ash silica	NCRHA
9	Polystyrene grafted commercial rice husk ash silica via enhanced spin capturing polymerization (ESCP) of styrene	PS-CRHA
10	Polystyrene grafted commercial rice husk ash silica via 1,3-dipolar cycloaddition of polystyrene macromonomer	PS-ene-CRHA

## **Materials**

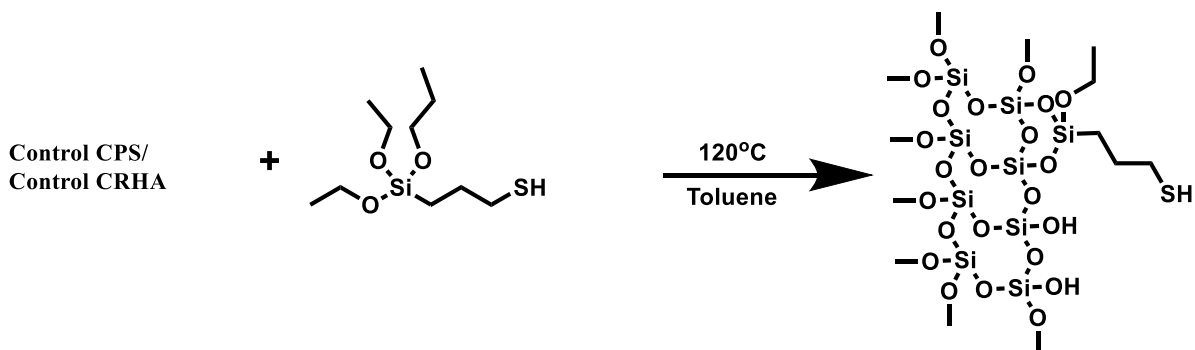
Sodium silicate (10 wt.%) was obtained from rice husk ash and commercial control rice husk ash silica was procured from Usher Eco Power Ltd., methacryloyl chloride was purchased from Avra Synthesis Pvt Ltd., 3-(mercaptopropyl)triethoxysilane (MPTES), 4-hydroxybenzaldehyde were purchased from TCI chemicals, nitrobenzene was purchased from RANKEM, and Zeosil 1165 was received from Solvay.

## **Characterization techniques**

Fourier transform infrared (FTIR) spectra were recorded in the spectral range of 400–4000  $\text{cm}^{-1}$  using a Thermo Nicolet IR 200 spectrometer. Thermogravimetric analysis (TGA) was performed till 850 °C from room temperature at a heating rate of 20 °C/minute using TA instruments SDT 650 under a nitrogen atmosphere. The UV-Visible spectra were recorded using Shimadzu 3600i plus UV Spectrophotometer. The morphological analyses were carried out via field emission scanning electron microscopy (FE-SEM) using JEOL JSM-7800F. The molecular weight was determined via size exclusion chromatography (SEC) analysis using Shimadzu Prominence. The solid-state NMR and XPS analysis was carried out using Jeol delta 400 MHz and Axis supra.

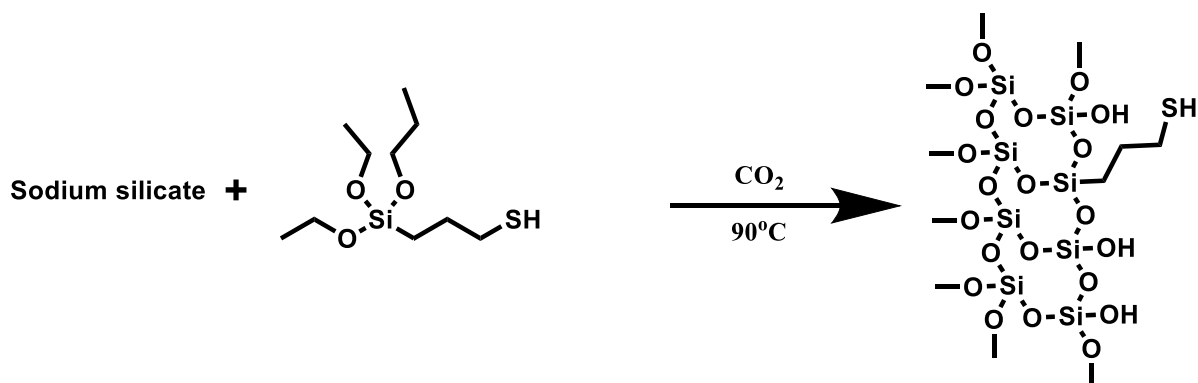
### ***S1. Synthesis of mercaptopropyl functionalized silica***

Mercaptopropyl functionalized silica has been synthesized over three different types of silica via co-condensation and post-modification methods. The post-modification method was used to synthesize the mercaptopropyl functionalized silica over control commercial precipitated silica (control CPS) and control commercial rice husk ash silica (control CRHA). 5 g of control silica was refluxed with 50 ml of toluene and 1 g (20 phr) of 3-(mercaptopropyl)triethoxysilane at 120 °C for 48 h. The functionalized samples obtained after the reaction were centrifuged and further washed with toluene to remove any unreacted silane.



Scheme S1. Synthesis of MCPS and MCRHA by post-modification

The co-condensation method of functionalization was used to synthesize the mercaptopropyl functionalized RHA silica particles, which involves one-step synthesis of functionalized silica by introducing silane during the precipitation followed by washing with water and ethanol to remove unreacted silane. The mercaptopropyl functionalized silica obtained was characterized using FTIR spectroscopy, TGA,  $^{13}\text{C}$  solid-state NMR spectroscopy.



Scheme S2. Synthesis of MRHA by co-condensation

### Determination of grafting density

The grafting density can be determined using the following **equation (1)**.

$$\text{Grafting density} \left( \frac{\mu\text{mol}}{\text{gm}} \right) = \frac{\left[ \left( \frac{W_s(100^\circ\text{C} - 800^\circ\text{C})}{100 - W_s(100^\circ\text{C} - 800^\circ\text{C})} \right) \times 100 - \left( \frac{W_p(100^\circ\text{C} - 800^\circ\text{C})}{100 - W_p(100^\circ\text{C} - 800^\circ\text{C})} \right) \times 100 \right]}{M_w \times 100} \times 10^6$$

Ws: weight loss of grafted sample.

Wp: weight loss of precursor sample. The precursor samples are control silica for mercaptopropyl functionalized silica, mercaptopropyl functionalized silica for nitrene functionalized silica, and nitrene functionalized silica for polystyrene grafted silica.

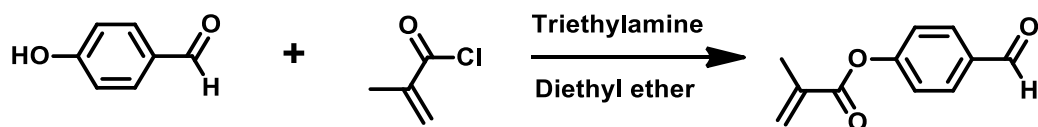
Mw: The molecular weight of organic fraction/grafted polymer

## ***S2. Synthesis of 4-(methacryloyloxy)benzaldehyde***

Synthesis of 4-(methacryloyloxy)benzaldehyde was carried out via the esterification reaction between 4-hydroxybenzaldehyde and methacryloyl chloride<sup>1</sup>. A solution of 4.9 g (0.04 mol) 4-hydroxybenzaldehyde in 150 ml of diethyl ether was prepared, and 11.4 ml (0.08 mol) triethylamine was added to the solution. The solution prepared was cooled down to 0 °C, followed by the dropwise addition of 8.4 g (0.08 mol) of methacryloyl chloride in 8 ml diethyl ether was carried out over 40 minutes. The resulting reaction mixture was further stirred for 6 h. The salt formed was filtered out, and the filtrate was refrigerated overnight. The salt further formed on the filtrate was filtered again and the filtrate was concentrated to obtain a pale-yellow solid product, and the obtained product was confirmed using <sup>1</sup>H NMR spectroscopy.

Esterification reaction between methacryloyl chloride and 4-hydroxybenzaldehyde in the presence of triethylamine was carried out for the synthesis of 4-(methacryloyloxy)benzaldehyde as shown in scheme S3. The salts formed were filtered out twice to ensure the purity and the product obtained was characterized using <sup>1</sup>H NMR spectroscopy (figure S1). The peaks correspond to the vinyl protons and the methyl group attached has been observed in the region of  $\delta=5.8$  ppm, 6.4 ppm, and 2.1 ppm with an integration value of 1:1:3. The peak corresponding to the aldehyde group has been observed in the region of  $\delta=10$  ppm and the integration value observed was in the ratio of 1:1 with respect to the vinylic proton confirms the formation of 4-(methacryloyloxy)benzaldehyde. Some side product formation has been observed in the region from  $\delta=1-2$  ppm, 2.2 ppm, and 3.8 ppm

which corresponds to dimer formed from methacryloyl chloride<sup>2</sup>, which can be removed in further condensation step for the nitron synthesis.



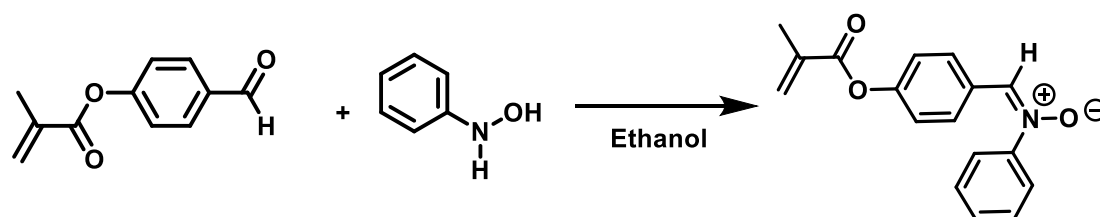
Scheme S3. Synthesis of 4-(methacryloyloxy)benzaldehyde

### S3. Synthesis of 4-(methacryloyloxy)benzaldehydephenylnitrone (*N*-(4-methacryloyloxybenzylidene)aniline *N*-oxide)

Freshly prepared 4.0 g (0.037 mol) phenylhydroxylamine<sup>3</sup> was added with 7.0 g of 4-(methacryloyloxy)benzaldehyde in 50 ml ethanol. The product was partially precipitated upon dissolving the reactant and the mixture was left overnight. The precipitated nitron was filtered, washed using ethanol and dried under vacuum to obtain 4-(methacryloyloxy)benzaldehydephenylnitrone. The obtained product was characterized using <sup>1</sup>H NMR, <sup>13</sup>C NMR and UV-visible spectroscopy.

The condensation reaction between freshly prepared phenylhydroxylamine<sup>3</sup> and 4-(methacryloyloxy)benzaldehyde in ethanol yields the 4-(methacryloyloxy)benzaldehydephenylnitrone as shown in scheme S4 and the product formed was precipitated in the reaction mixture. The product precipitated was filtered under vacuum and further washed with fresh ethanol and dried under vacuum. The <sup>1</sup>H NMR spectra obtained for 4-(methacryloyloxy)benzaldehyde phenylnitrone shows the characteristic peak at  $\delta=8$  ppm corresponding to (CH=N-O) with the disappearance of aldehyde peak at  $\delta=10$  ppm confirming the formation of nitron functionality (figure S2). The peaks corresponding to vinylic proton with the attached methyl group can also be observed at  $\delta=5.8$  ppm, 6.4 ppm, and 2.1 ppm along with the aromatic peaks in the range of  $\delta=7.3$  ppm, 7.6 ppm, 7.8 ppm, and 8.5 ppm. The UV-visible spectroscopy observed for 4-(methacryloyloxy)benzaldehyde phenylnitrone (figure S4)

confirms the presence of nitron functionality with the peak observed at  $\lambda = 327$  nm along with the peak corresponding to the aromatic group attached at  $\lambda = 242$  nm. Thermogravimetric analysis obtained under nitrogen atmosphere (figure S4) shows an onset degradation of  $256$  °C with a char yield of 25 %. The 4-(methacryloyloxy)benzaldehyde phenylnitron synthesized was further used for the synthesis of nitron-functionalized silica particles.



Scheme S4. Synthesis of 4-(methacryloyloxy)benzaldehyde phenylnitron.

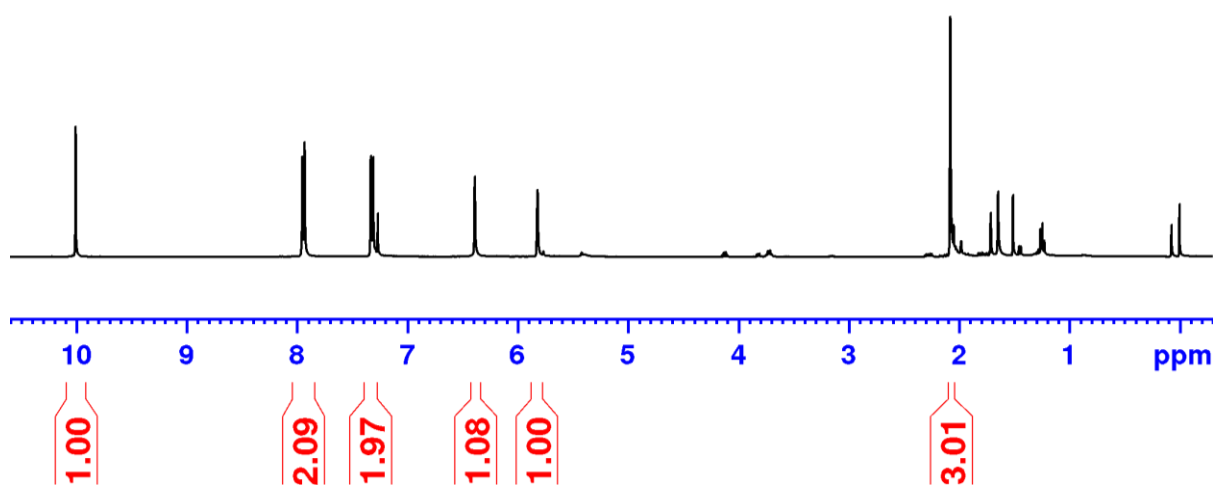


Figure S1.  $^1\text{H}$  NMR spectrum of 4-(methacryloyloxy)benzaldehyde.

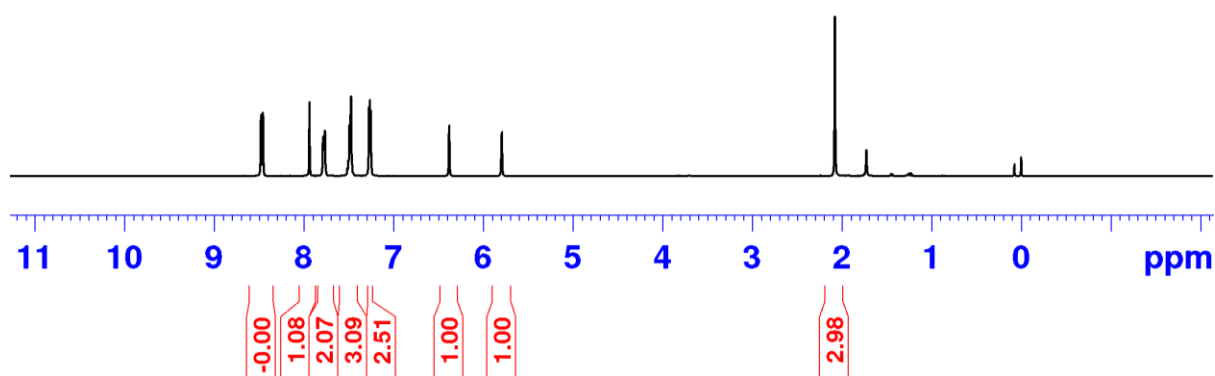


Figure S2.  $^1\text{H}$  NMR spectrum of 4-(methacryloyloxy)benzaldehyde phenylnitrone.

The  $^{13}\text{C}$  NMR spectra obtained also confirmed the formation of 4-(methacryloyloxy)benzaldehyde phenylnitrone with the presence of peaks corresponding to the aromatic region from  $\delta=120$  ppm to 150 ppm along with the peaks corresponding to vinylic carbon atom at  $\delta=130$  (figure S3). The peak corresponding to the methyl carbon attached to the vinylic group was observed at the range of  $\delta=19$  ppm and the peak corresponding to the ester group attached was observed at  $\delta=166$  ppm. The peak corresponding to the carbon atom ( $\text{CH}=\text{N}-\text{O}$ ) was not observed in the  $^{13}\text{C}$  NMR spectra despite of observing signal at  $^1\text{H}$  NMR spectra, possibly due to the lower abundance and fewer nearby protons.

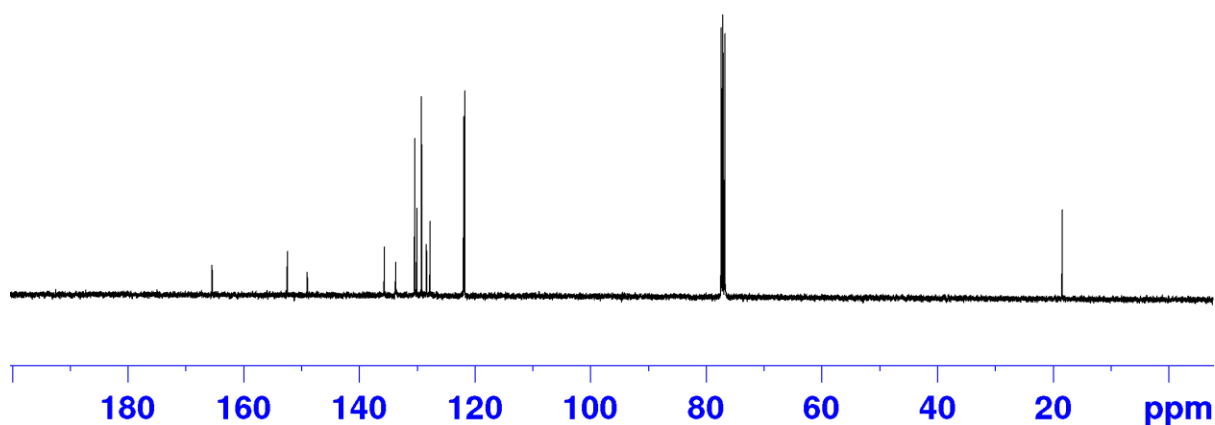


Figure S3.  $^{13}\text{C}$  NMR spectrum of 4-(methacryloyloxy)benzaldehyde-phenylnitrone.

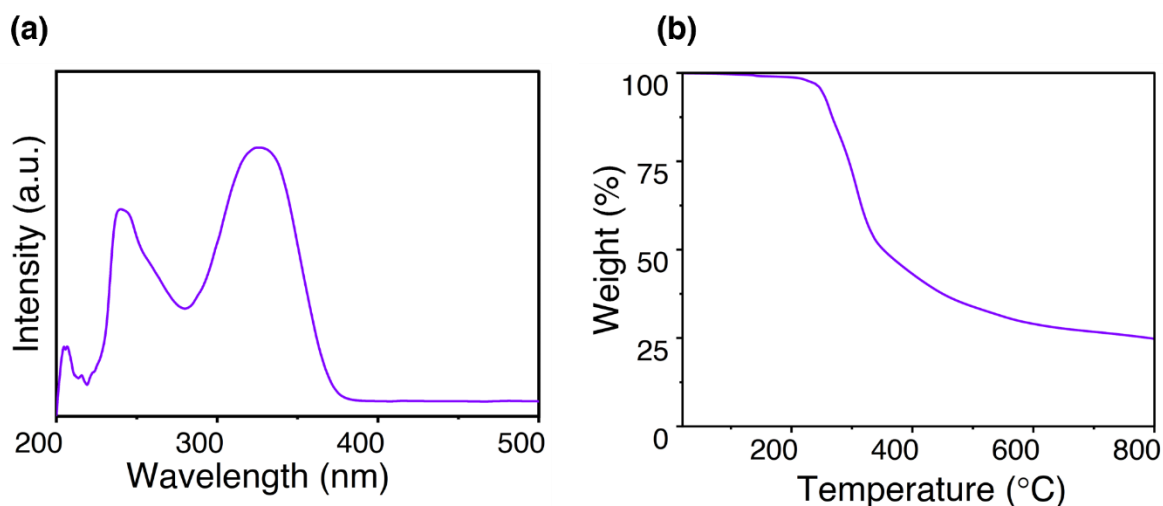


Figure S4. (a) UV-visible spectra and (b) TGA plot for 4-(methacryloyloxy)benzaldehyde-phenylnitrone.

The structural characterization of nitron functionality over silica surface has been carried out via  $^{13}\text{C}$  solid-state NMR analysis of nitron functionalized RHA silica (NRHA) and mercaptopropyl functionalized RHA silica (MRHA) samples (figure S5). The characteristic peak to confirm the thiol-ene reaction was observed at  $\delta=51$  ppm along with the aromatic peaks in the region of  $\delta=111$ -138 ppm. The intensity observed for the aromatic region was lower due to the minimal grafting density and the peaks corresponding to the ester carbon as well as the nitrogen attached carbon atom ( $\text{CH}=\text{N}-\text{O}$ ) were also not observed due to the limited number of neighbouring protons

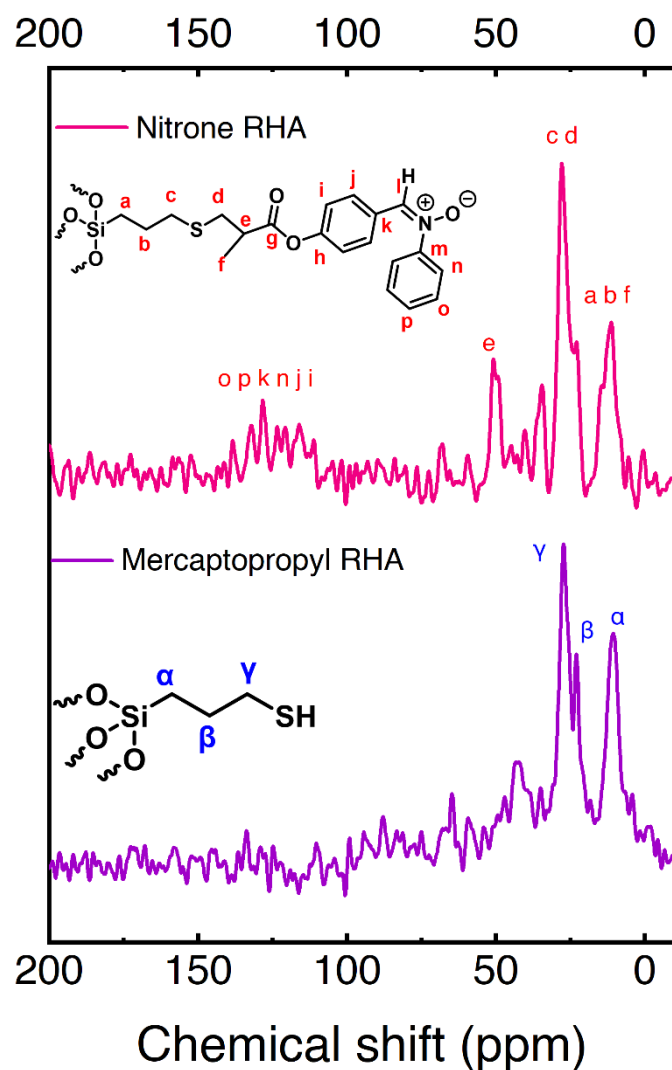


Figure S5.  $^{13}\text{C}$  solid-state NMR spectra of mercaptopropyl functionalized RHA and nitrone functionalized RHA silica.

#### ***S4. Nitrone functionalized RHA silica***

The nitrone-functionalized silica was synthesized via thiol-ene reaction between mercaptopropyl functionalized silica and 4-(methacryloyloxy)benzaldehyde phenylnitron using triphenylphosphine in 1:1 methanol and THF solvent mixture (scheme 1). The polarity of THF was not sufficient to carry forward the reaction and the 4-(methacryloyloxy)benzaldehyde phenylnitron was insoluble in methanol. The mixture of

solvents helped in carrying the reaction forward, however, the progress of reaction observed was slower (~24% at 14 h) when monitored using  $^1\text{H}$  NMR for mercaptopropyl triethoxysilane and 4-(methacryloyloxy)benzaldehyde phenylnitrone. The reaction on the surface was carried out for 72 h to provide maximum progress over thiol-ene reaction yielding 37% of surface MPTES conversion.

The qualitative confirmation of polystyrene grafted on nitrone functionalized RHA was performed using FTIR analysis and the bands corresponds to aromatic C-H stretching observed at  $3022\text{ cm}^{-1}$  and out of plain C-H bending was observed at  $694\text{ cm}^{-1}$  (figure 3). The alkyl C-H bending was  $1457\text{ cm}^{-1}$  along with the aliphatic C-H stretching vibration at  $2928\text{ cm}^{-1}$  and the vibrations of Si-O-Si were also observed in the FTIR spectra. The intensity of aromatic C-H stretching and out of plain C-H bending was observed to be increasing with increase in conversion, which qualitatively indicates the increase in grafting density with respect to the conversion.

The thermogravimetric analysis of nitrone functionalized silica samples was showing a degradation pattern from  $100\text{ }^\circ\text{C}$  despite of the  $260.2\text{ }^\circ\text{C}$  onset degradation of 4-(methacryloyloxy)benzaldehyde phenylnitrone, possibly due to the hydrolysis of nitrone functionality due to the acidic silica surface. The decomposition of nitrone functionality on the surface of silica can also be observed visually by leaving the nitrone-functionalized silica at  $100\text{ }^\circ\text{C}$  overnight, which changes the colour of silica to black from light green. The grafting density hence was calculated by accounting the weight loss from the region of  $100\text{ }^\circ\text{C}$  to  $850\text{ }^\circ\text{C}$ . In addition, due to the limited stability of nitrone-functionalized silica under higher temperature, all the polymer grafting, and handling of the functionalized samples were carried out at the temperature below  $100\text{ }^\circ\text{C}$ .

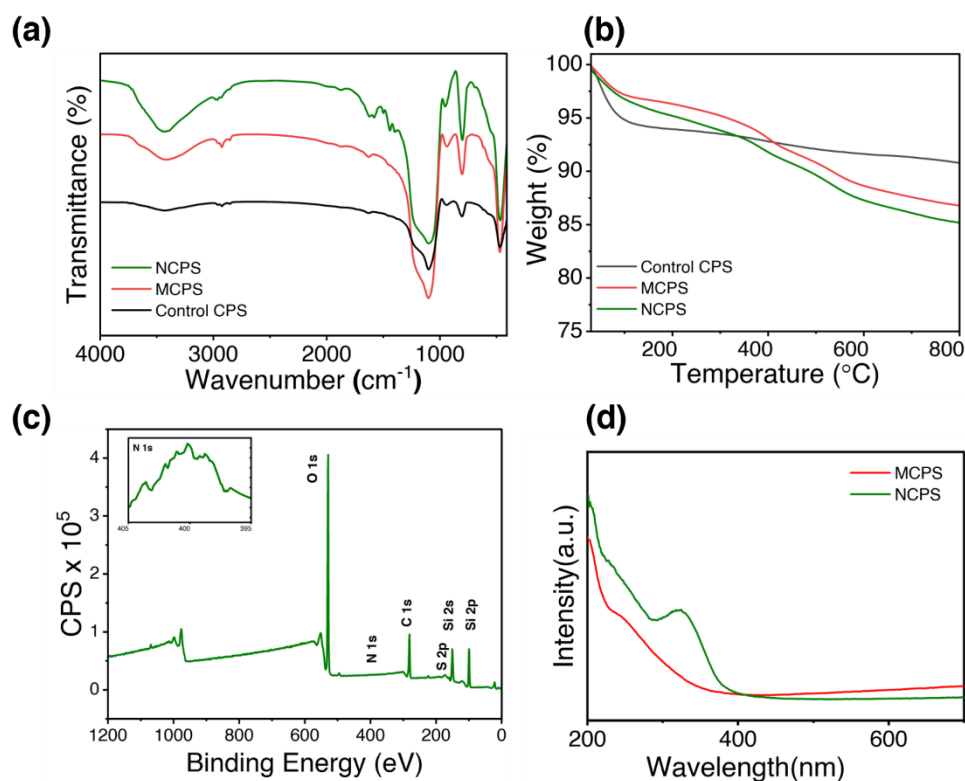


Figure S6. (a) FTIR and (b) TGA analysis of control CPS silica, MCPS and NCPS silica (c) XPS spectra of NCPS silica (d) UV-visible spectra of MCPS and NCPS silica.

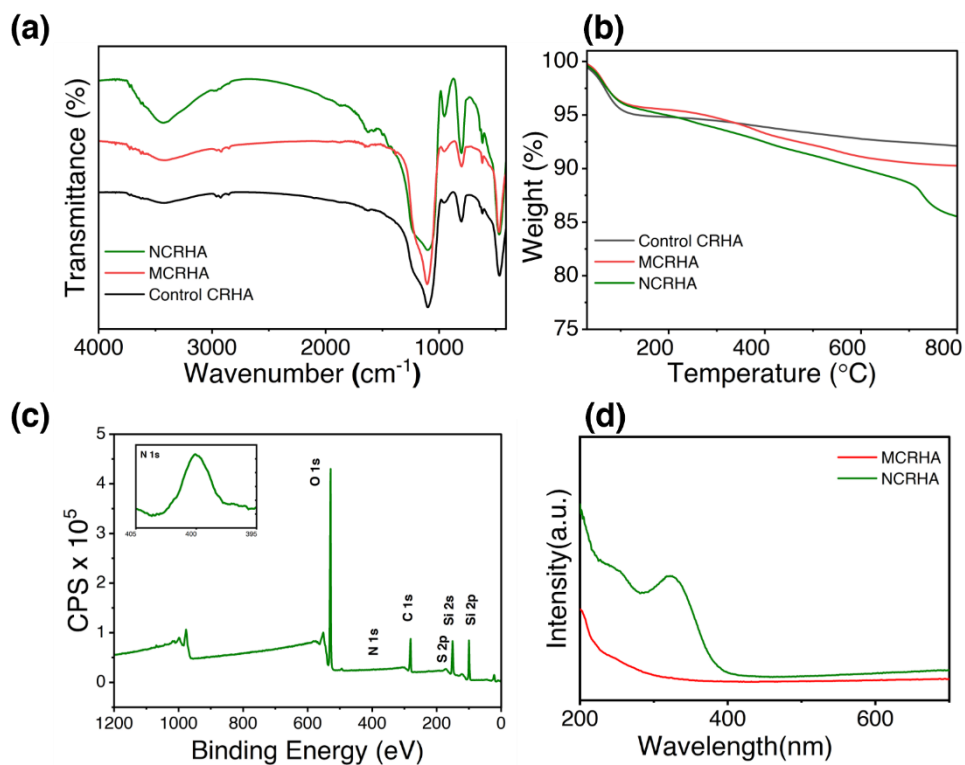


Figure S7. (a) FTIR and (b) TGA analysis of control CRHA silica, MCRHA and NCRHA silica(c) XPS spectra of NCRHA silica (d)UV-visible spectra of MCRHA and NCRHA silica.

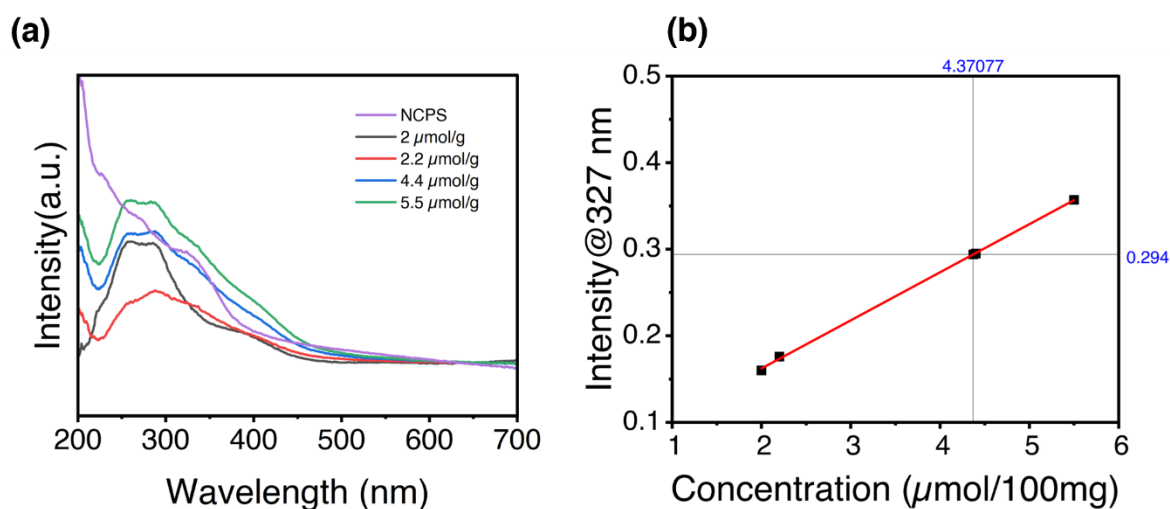


Figure S8. Nitrene grafting density determined using solid-state UV analysis for NCRHA silica.

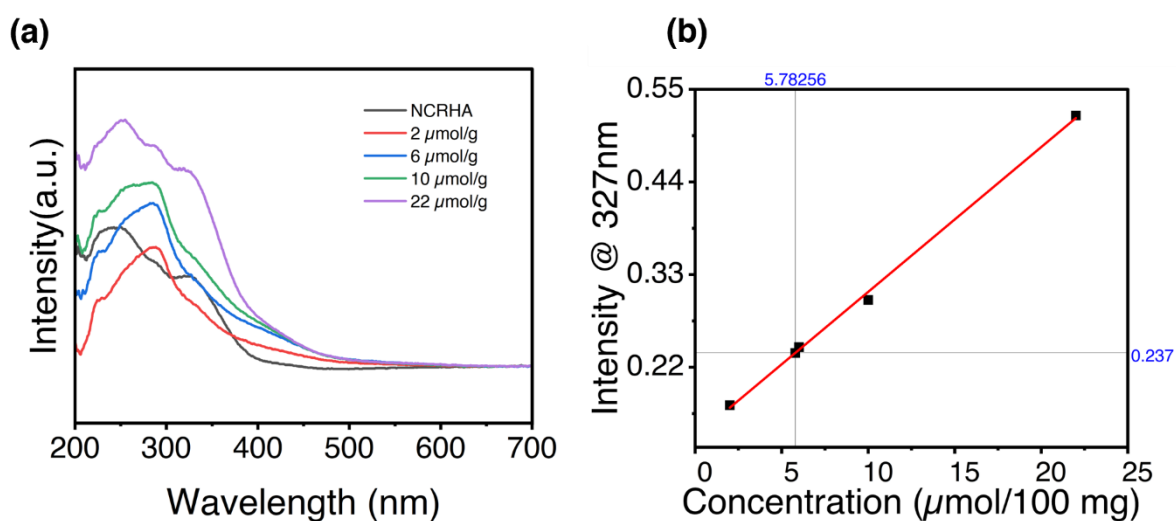


Figure S9. Nitrene grafting density determined using solid-state UV-visible spectroscopy for NCRHA silica.

### S5. Nitrene RHA XPS discussion

The introduction of nitrene functionality over mercaptopropyl functionalized silica increased the intensity of C1s peak along with the slight shift towards the lower binding energy region

which corresponds to the aromatic C=C bonds (figure S10), however the quantification of nitrene functionality with respect to the added aromatic carbons were not yielding accurate data due to the inconsistent carbon ratios in mercaptopropyl functionalized samples (figure S11).

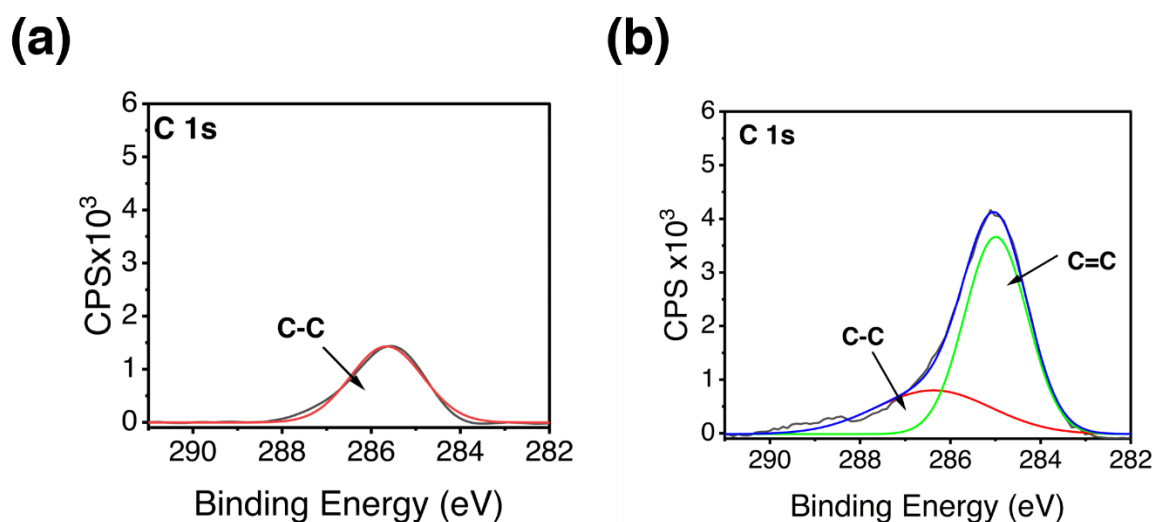


Figure S10. C1s narrow scan for (a) mercaptopropyl RHA and (b) Nitrene RHA using XPS analysis.

The carbon to sulphur ratio for mercaptopropyl functionalized samples itself shows a significant variation in carbon percentage, possibly due to the partial condensation of ethoxy silanes or due to the organic impurity such as lignin and cellulose in RHA silica due to its bio-origin<sup>2</sup>. In addition, the reason may also be due the procedure used for the preparation of mercaptopropylsilane functionalized RHA silica. For the preparation of mercaptopropyl functionalized silica co-condensation approach was used and not surface modification. XPS is highly sensitive technique for characterization of surfaces, and it is not a bulk characterization technique. The nitrogen to sulphur ratios determined using XPS analysis were observed to be higher than the ratio determined from the grafting density using both TGA and solid-state UV-

visible spectroscopy. The nitrogen to sulphur ratio obtained from TGA and solid-state UV-visible spectroscopy was 0.32, whereas the ratio obtained using XPS analysis was 0.43.

*[The mercaptopropyl grafting density was 663  $\mu\text{mol/g}$  and the nitrene grafting density was 215  $\mu\text{mol/g}$  using TGA and solid-state UV-visible spectroscopy. The elemental percentage obtained for sulphur was 0.3% and for nitrogen was 0.7 % in XPS analysis.]*

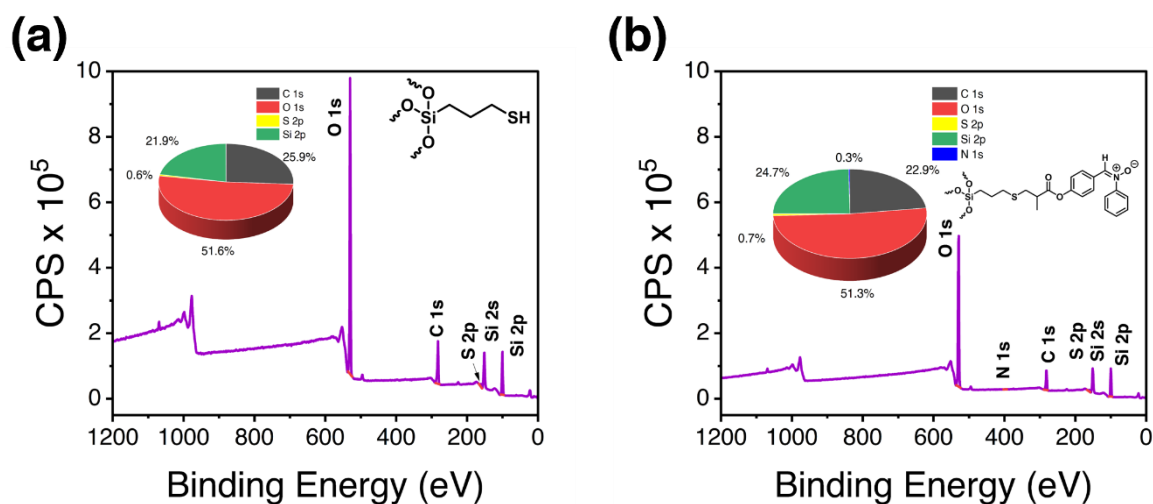


Figure S11. Wide scan and C, S, N percentage for (a) Mercaptopropyl RHA and (b) Nitrene RHA using XPS analysis.

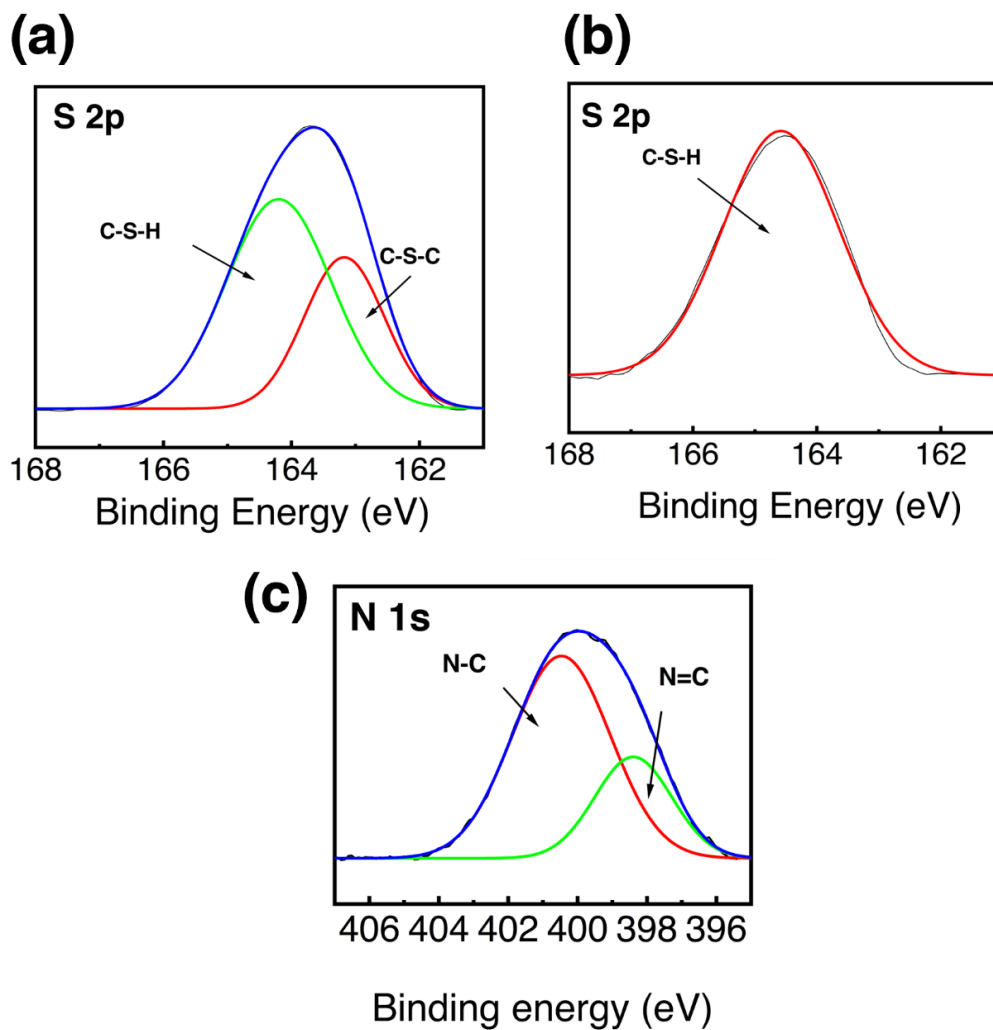


Figure S12. (a) S2p narrow scan for Nitron RHA (b) S2p narrow scan for mercaptopropyl RHA using XPS analysis and (c) N1s narrow scan for Nitron RHA.

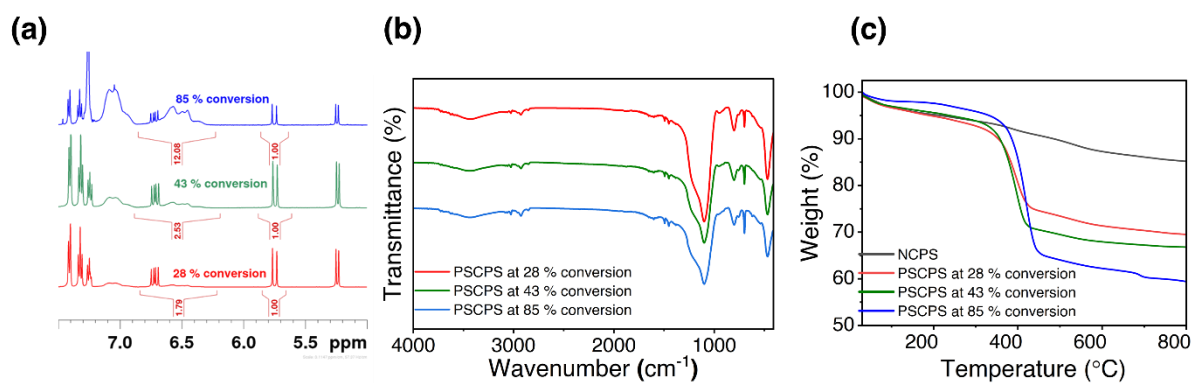


Figure S13. (a)  $^1\text{H}$  NMR, (b) FTIR (c) TGA graphs for PSCPS synthesized via ESCP at 28 %, 43 % and 85 % conversion

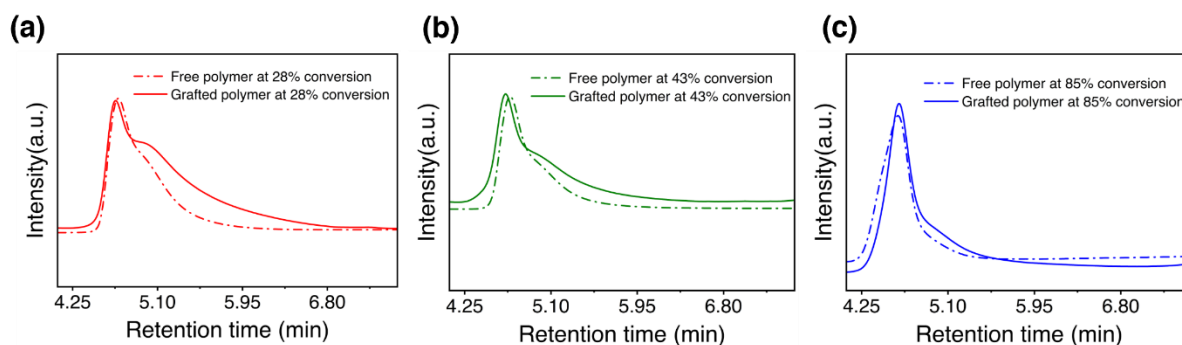


Figure S14. SEC traces for free polymer from solution (FP) and cleaved grafted polymer from surface (GP) of PSCPS silica synthesized via ESCP at (a) 28 % conversion, (b) 43 % conversion (c) 85 % conversion.

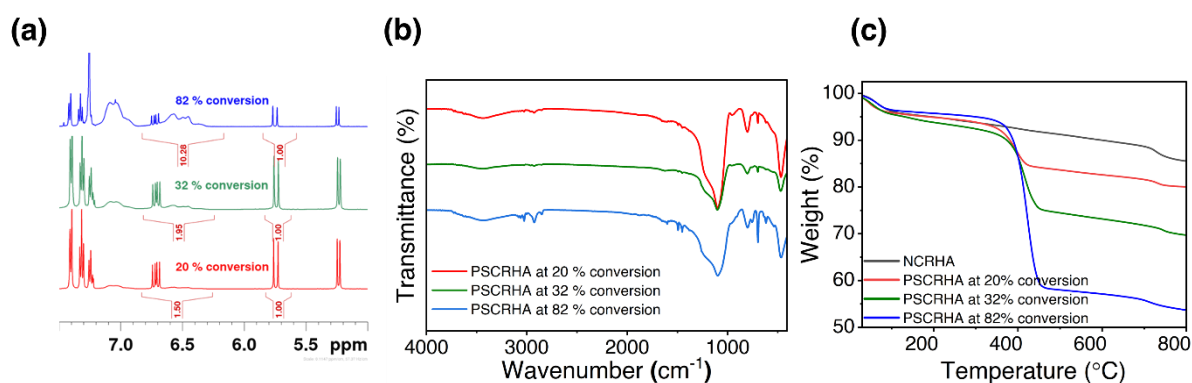


Figure S15. (a)  $^1\text{H}$  NMR, (b) FTIR (c) TGA graphs for PSCRHA synthesized via ESCP at 20 %, 32 % and 82 % conversion

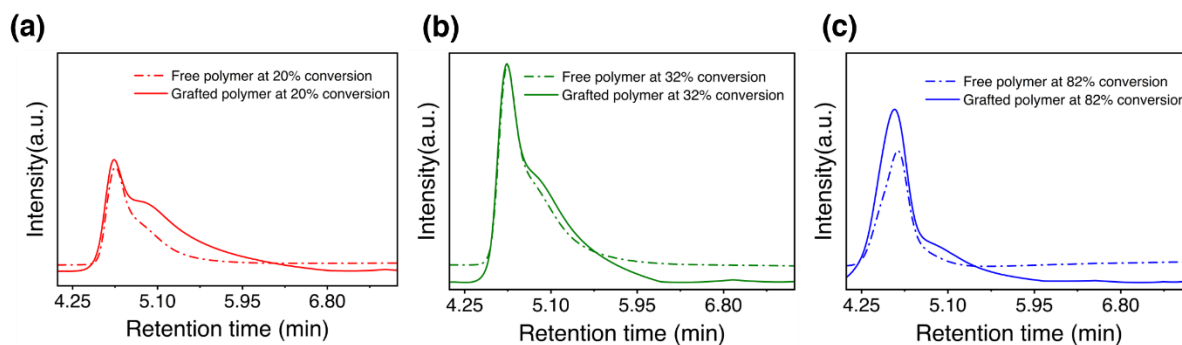


Figure S16. SEC traces for free polymer from solution (FP) and cleaved grafted polymer from surface (GP) of PSCRHA silica synthesized via ECPS at (a) 20 % conversion, (b) 32 % conversion, (c) 82 % conversion.

### ***S6. Polymer grafting studies over nitrene-functionalized commercial silica particles via enhanced spin capturing polymerization***

The PSCPS samples were synthesized at three different conversions of 28 %, 43 % and 85 % and the grafted samples observed were characterized using FTIR spectroscopy. The characteristic bands observed for the aromatic C-H stretching vibration at  $3022\text{ cm}^{-1}$  along with the increase in out of plain C-H bending observed at  $700\text{ cm}^{-1}$  with increase in conversion qualitatively confirms the polystyrene grafting along with the increase in polystyrene grafting with increase in conversion. TGA analysis quantitatively confirm the increase in polymer grafting with increase in conversion with 14.86 %, 18.56 %, 27.62 % weight loss attributed to the grafted polystyrene for 28 %, 43 % and 85 % conversions respectively. The SEC trace observed (figure S12) for the free polymer at a conversion of 28 % was 44000 g/mol with dispersity of 1.25 whereas the grafted polymer molecular weight observed to be decreased to 28000g/mol with an increase in dispersity of 1.65. Similar trend has been observed for the polymers at 85 % conversion where the molecular weight for grafted polymer obtained was 59000 g/mol with dispersity 1.35 from that of free polymer 84000g/mol with dispersity of 1.17. A slight decrease in the molecular weight of grafted polymer chain has observed for the conversion 43% in the range of 47000 g/mol with increase in in dispersity of 1.35 from 1.26. The reduction in molecular weight of grafted chain with increase in  $\bar{M}_w$  value indicates the polymer grafting over nitrene functionality in NCPS throughout the propagation step.

The PSCRHA samples were prepared at the conversions of 20 %, 32 % and 82 % conversions. The bands correspond to aromatic C-H stretching at  $3022\text{ cm}^{-1}$  and C-H out of plain bending

vibration at  $688\text{ cm}^{-1}$  confirms the polystyrene grafting over NCRHA surfaces. The quantitative analysis using TGA indicates the organic weight loss corresponds to grafted polystyrene observed was 5.23 %, 14.79 %, and 32.74 % for 20 %, 32 % and 82 % conversions respectively. The increase in weight loss corresponds to the increase in conversion indicates the increased polystyrene grafting with respect to the conversion. The molecular weight obtained by SEC analysis indicates the reduction in molecular weight of grafted polymer with respect to the free polymer throughout all the conversions. The molecular weight was reduced for conversion at 20 % was from 50000 g/mol for free polymer to 36000 g/mol for grafted polymer with an increase in dispersity value from 1.24 to 1.46. At 32 % conversion, the molecular weight observed for the grafted polymer was 37000 g/mol with dispersity of 1.48 from that of free polymer with 48000 g/mol with dispersity 1.29. The molecular weight for grafted polymer with conversion 82 % was observed 77000 g/mol with a dispersity of 1.30 whereas the molecular weight observed for the free polymer was observed at 90000 g/mol with a dispersity of 1.12. The reduction in molecular weight with respect to the free polymer along with the increase in dispersity value indicates the presence of polymer grafted via nitrene functionality throughout the polymerization.

### ***S7. Synthesis of polystyrene macroinitiator via atom transfer radical polymerization***

Polystyrene macroinitiator was synthesized via atom transfer radical polymerization (ATRP) method<sup>4</sup>. 50 ml of styrene, 143 mg of copper(I)bromide (CuBr) were added to a 100 ml RB flask. The solution was purged for 30 minutes under nitrogen in an ice bath. Degassed 112  $\mu\text{L}$  of methyl-2-bromopropionate (MBrP) and 418  $\mu\text{L}$  of pentamethyldiethylenetriamine (PMDETA) were added to the flask via degassed syringe. The reaction mixture was heated at 100 °C for 40 minutes. The polymerization was stopped by dipping the flask in ice bath followed by opening it to air. The reaction mixture was poured into a beaker containing 500 mg of copper(II)bromide (CuBr<sub>2</sub>) and left overnight under vacuum to remove the unreacted

styrene. The reaction mixture was further diluted by adding THF and purified from copper complexes by passing through silica column. The polymer solution was concentrated and precipitated in cold methanol and dried under vacuum. The polymer obtained was characterized using  $^1\text{H}$  NMR spectroscopy and SEC analysis.

### ***S8. Synthesis of polystyrene macromonomer***

The HBr elimination of bromine terminated polystyrene synthesized via ATRP method yields ene terminated polystyrene macromonomer<sup>5</sup>. 3 g of bromine terminated polystyrene was dissolved in 10 ml of DMF. The mixture was purged under nitrogen for 30 minutes. The reaction mixture was stirred at 100 °C for 16 h. The reaction mixture was cooled down and ethyl acetate was added and followed by washing with distilled water four times. The organic phase was dried using sodium sulphate, filtered, concentrated, and precipitated in methanol. The polymer precipitated was filtered and dried under vacuum to obtain ene functionalized polystyrene. The polystyrene macromonomer obtained was characterized using  $^1\text{H}$  NMR spectroscopy.

The removal of bromine end group and the formation of ene functionality was confirmed via  $^1\text{H}$  NMR analysis (refer supplementary information figure S17). The disappearance of peak corresponds to the proton attached to the bromine end group at  $\delta= 4.5$  ppm and the formation of peak corresponds to the vinylic proton at  $\delta= 6.1$  ppm with change in integration ratio from 1:2 confirms the formation of polystyrene macromonomer. The molecular weight distribution of polystyrene macromonomer were determined using SEC analysis and compared to polystyrene macroinitiator (refer supplementary information figure S18).

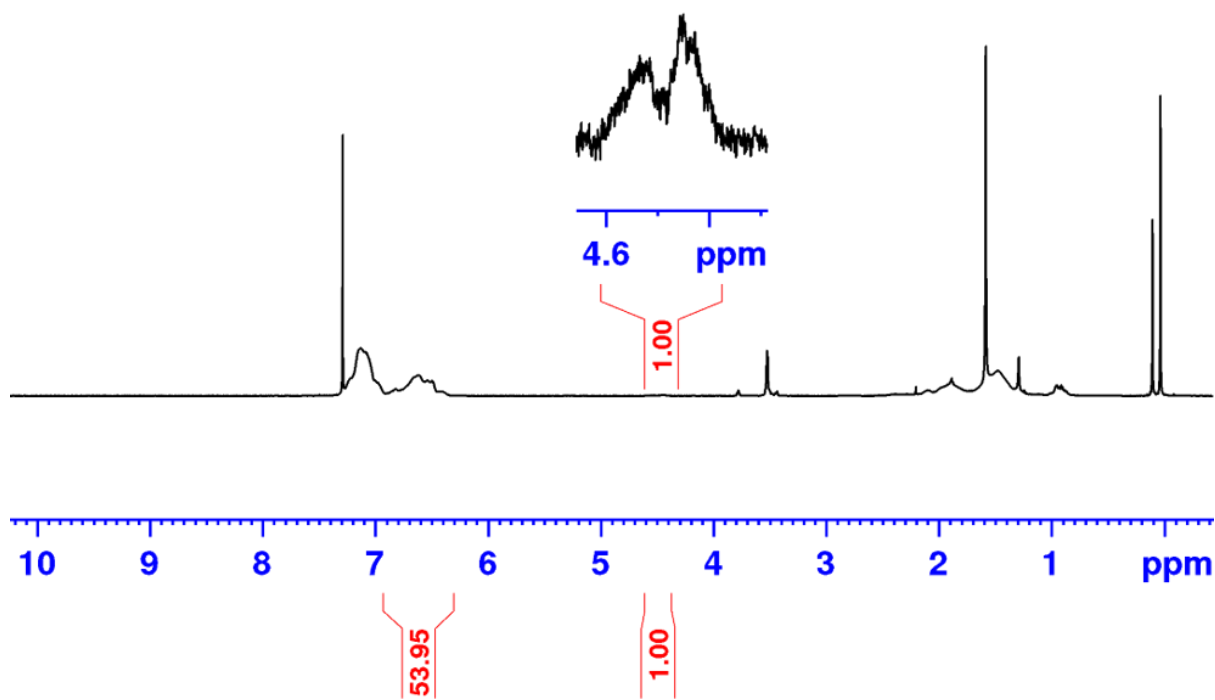


Figure S17.  $^1\text{H}$  NMR spectrum of bromine terminated polystyrene.

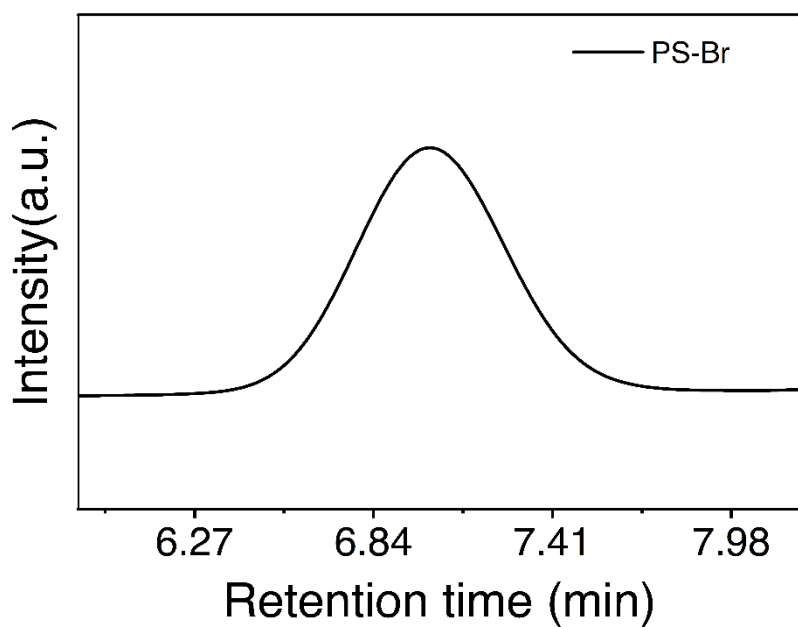


Figure S18. SEC traces of bromine-terminated polystyrene.

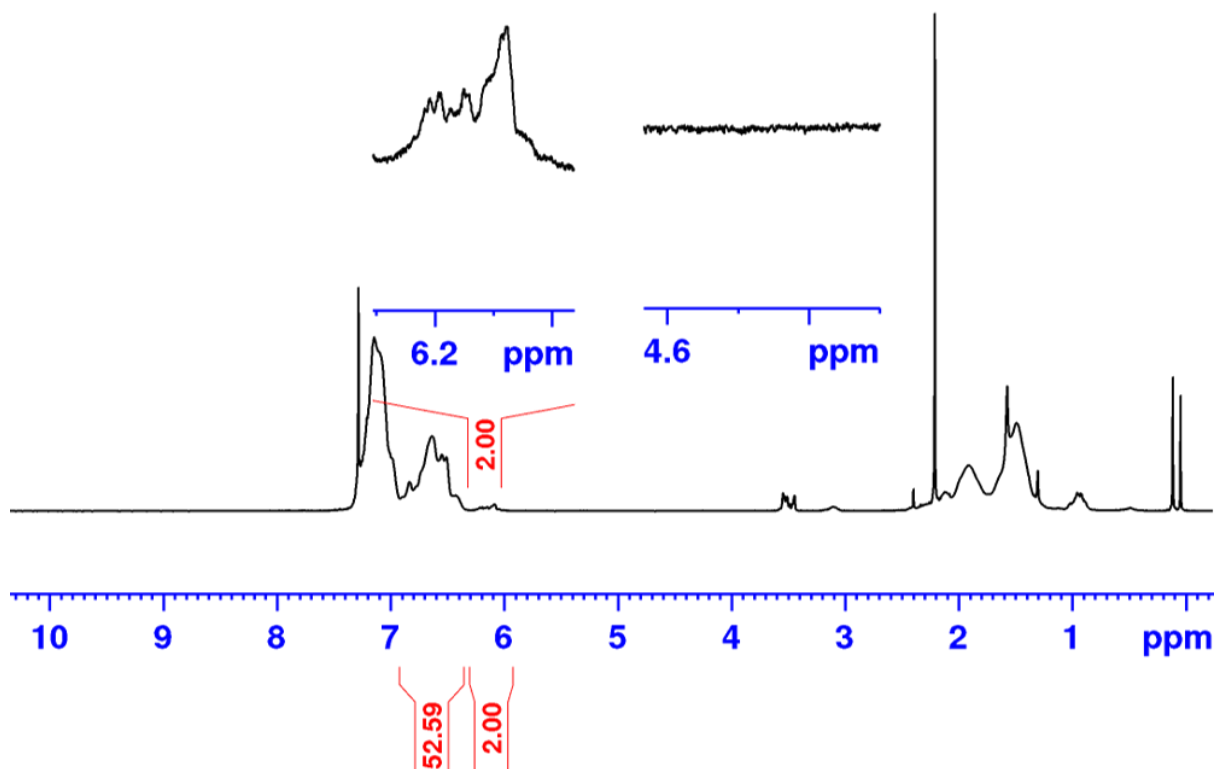


Figure S19.  $^1\text{H}$  NMR spectrum of polystyrene macromonomer.

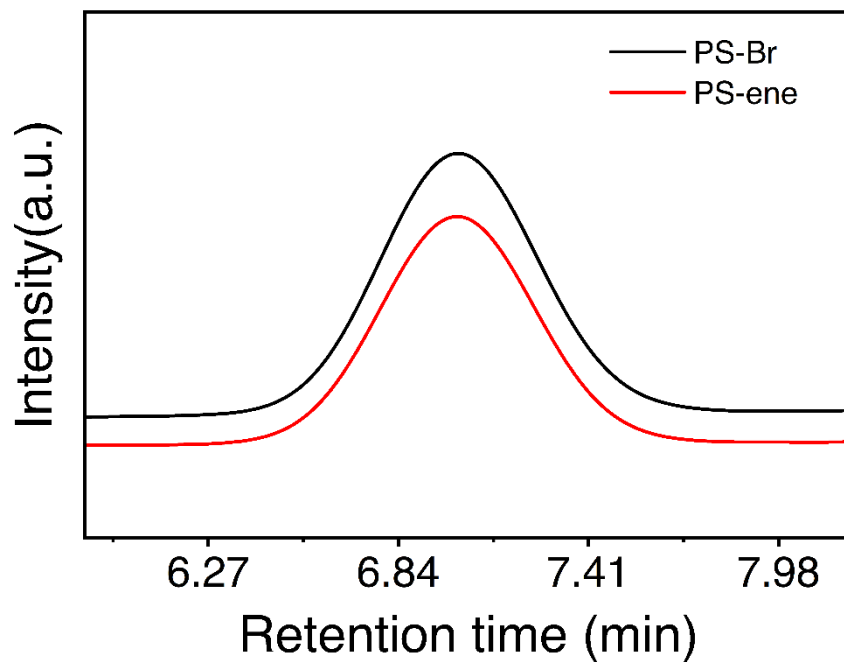


Figure S20. SEC traces for polystyrene macroinitiator and polystyrene macromonomer.

Table S2. Molecular weight and grafting density of polymer grafted nitrene-functionalized silica via 1,3-dipolar cycloaddition of polystyrene macromonomer. The polystyrene

macroinitiator was synthesized via ATRP method and the HBr elimination of macroinitiator yields the polystyrene macromonomer. The molecular weight of macroinitiator and macromonomer was determined using SEC analysis. The TGA weight loss due to the grafted polystyrene macromonomer was determined by adjusting the organic weight loss of nitrene-functionalized silica samples. The molecular weight of grafted polystyrene was determined via SEC analysis by cleaving the grafted polystyrene from the surface. The grafting density was determined in  $\mu\text{mol/g}$  unit due to the inconsistent surface area of RHA silica due to higher agglomeration and the grafting density was determined using equation 1

<b>Sample</b>	<b>Mn Polystyrene macroinitiator (g/mol) / Dispersity</b>	<b>Mn Polystyrene macromonomer (g/mol) / Dispersity</b>	<b>TGA weight loss due to grafted polymer (%)</b>	<b>Mn GP (g/mol) / Dispersity</b>	<b>Grafting density (<math>\mu\text{mol/g}</math>)</b>
<b>PS-eneRHA</b>	2600/1.08	2600/1.08	1.78	2600/1.07	6.8

### *S9. Model 1,3 dipolar cycloaddition reactions*

Model 1,3 dipolar cycloaddition reaction of styrene was carried out with N-1-diphenylmethanimine oxide synthesized using benzaldehyde and phenylhydroxylamine. Equimolar amount of styrene and benzaldehyde phenylnitrene was refluxed in toluene at 80 °C for 16 h. The resulting product was concentrated, dried under vacuum, and  $^1\text{H}$  NMR spectroscopy was performed analysis to monitor the cycloaddition reaction.

Model 1,3 dipolar cycloaddition of nitrene-functionalized polystyrene and polystyrene macromonomer was carried out in similar manner. The nitrene-functionalized polystyrene was synthesized using the thiol-ene reaction between -SH functionalized polystyrene with 4-(methacryloyloxy)benzaldehyde phenylnitrene using triphenylphosphine. The -SH functionalized polystyrene has been synthesized using the aminolysis of polystyrene synthesized using RAFT (reversible addition fragmentation chain-transfer polymerization)

polymerization. The precipitated polymer samples were dried and characterized using SEC and  $^1\text{H}$  NMR spectroscopy.

Model 1,3 dipolar cycloaddition over nitrene functionalized silica was carried out using isobornyl acrylate. 100 mg of nitrene functionalized RHA silica samples were dispersed in the mixture of 0.2 ml of isobornyl acrylate and 1 ml toluene. The reaction mixture was refluxed 80 °C overnight. The silica samples were repeatedly washed with toluene, dried in vacuum oven at 50 °C and characterized using FTIR, TGA and solid-state UV-visible spectroscopy.

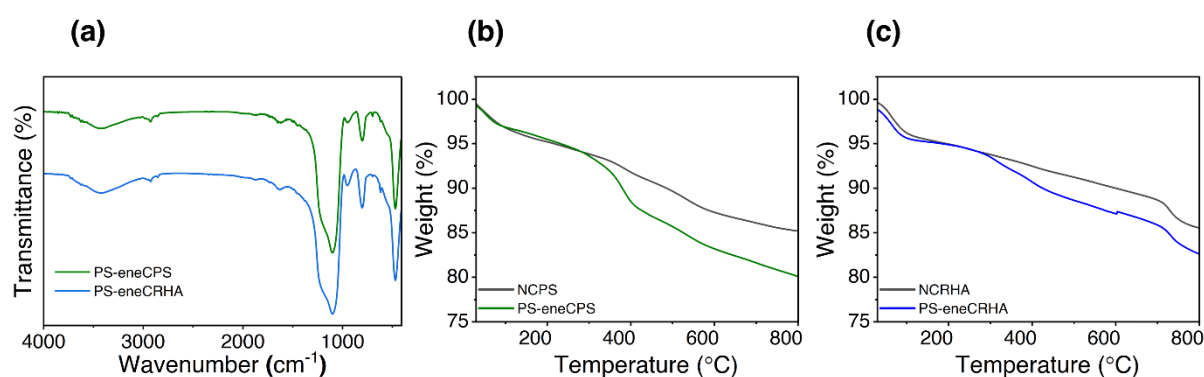


Figure S21. (a) FTIR spectra for PS-eneCPS, and PS-eneCRHA. (b) TGA graph for NCPS and PS-eneCPS silica (c) TGA graph for NCRHA and PS-eneCRHA silica.

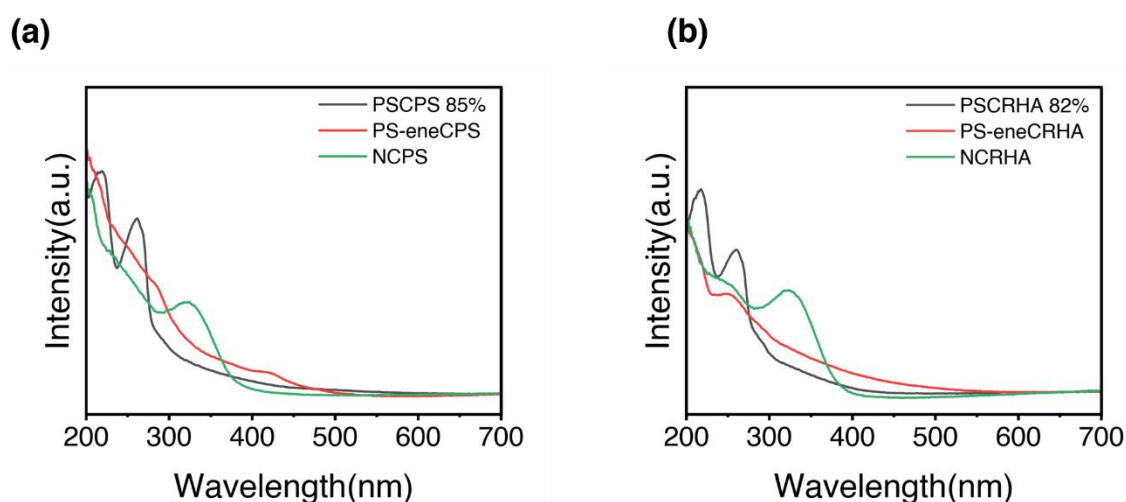


Figure S22. UV-visible spectra for nitrene functionalized silica (a) NCPS and (b) NCRHA after polymer grafting studies via ESCP and 1,3-dipolar cycloaddition of PS-ene.

### ***S10. Discussion on polymer grafting density***

Since the silica samples possess very high agglomeration, the surface area determined is not accurate which we have observed for the case of control CRHA samples. The surface area was drastically increased from 70 m<sup>2</sup>/g for control CRHA to 229 m<sup>2</sup>/g upon surface modification. Due to the inconsistency in determined surface area, the grafting density was calculated based on weight of silica samples. For PSRHA samples at 25 % conversion, the molecular weight of the grafted polymer was observed to be double as compared to the free polymer molecular weight, possibly due to the grafting of two growing polymers on one nitrene functionality. Hence the determination of grafting density at 25% conversion is carried out by assuming the free polymer molecular weight to the grafted polymer chain. The grafting density of PSRHA observed to be increasing from 3.4 μmol/g to 9.1 μmol/g from 25 % to 68 % conversion followed by reduced to 6.8 μmol/g at 80% conversion. The PSCPS samples shows a high grafting density of 7.5 μmol/g at the lowest conversion of 28 % compared to PSRHA and PSCPS silica samples followed by reduced to 5.3 μmol/g and 5.7 μmol/g at 43 % and 85 % conversions. The PSCRHA samples on the other hand shows the lowest initial grafting density of 2.8 μmol/g at 20 % conversion followed by increased to 5.3 μmol/g and 4.9 μmol/g at 32 % and 82 % conversion (figure 7). The reduction of grafting density observed at very high conversion is possibly due to the restricted mobility of growing polymer particles to quench on surface of silica due to the increases in viscosity and chain entanglement. For polymer grafting via 1,3-dipolar cycloaddition, PS-eneCPS samples observed to have a very high grafting density of 21.9 μmol/g followed by PS-eneCRHA 9.1 μmol/g. The PS-eneRHA samples observed to have the grafting density of 6.8 μmol/g.

Table S3. Molecular weight and grafting density of polymer grafted nitrene functionalized silica.

Sample	Conversion (%)	TGA weight loss due to grafted PS (%)	Mn FP (g/mol) / Dispersity	Mn GP (g/mol) / Dispersity	Grafting density ( $\mu\text{mol/g}$ )
PSRHA	25	13.05	38000/1.34	85000/1.07 3500/1.09	3.4
	68	26.14	52000/1.24	29000/1.56	9.1
	80	37.88	81000/1.15	56000/1.35	6.8
PSCPS	28	21.13	44000/1.27	28000/1.65	7.5
	43	24.83	47000/1.26	47000/1.35	5.3
	85	33.89	84000/1.17	59000/1.35	5.7
PSCRHA	20	10.09	50000/1.24	36000/1.46	2.8
	32	19.65	48000/1.29	37000/1.48	5.3
	82	37.6	90000/1.12	77000/1.30	4.9
PS-eneRHA	-	1.78	-	2600/1.07	6.8
PS-eneCPS	-	5.7	-	2600/1.07	21.9
PS-eneCRHA	-	2.36	-	2600/1.07	9.1

***S11. Effect of silica surface area and method of surface functionalization on grafting density***

The surface area was determined using Brunauer–Emmett–Teller (BET) analysis. The determination of surface area for a nitrene modified silica samples was observed to yield 170  $\text{m}^2/\text{g}$ , 114  $\text{m}^2/\text{g}$  and 67  $\text{m}^2/\text{g}$  for NRHA, NCPS and NCRHA respectively. The drastic reduction in the surface area observed compared to the precursors is possibly due to the agglomeration of nitrene functionalized silica samples in the bulk state. The actual surface area of NRHA and NCRHA silica system was used from the surface area of the precursor samples by the modification with small nitrene molecules will not hamper the surface area drastically. The surface area observed for functionalized RHA silica was 280  $\text{m}^2/\text{g}$ . The functionalized CRHA silica possess the surface area of 229  $\text{m}^2/\text{g}$  and the control CPS silica samples claim to have the surface area of 165  $\text{m}^2/\text{g}$  from the manufacturer. The surface area observed was in the order of NRHA>NCRHA>NCPS. The increased surface area of NRHA samples observed to have increase in polymer grafting at 68% conversion. On the other hand, the NCPS samples shows

higher grafting density of 7.5 m<sup>2</sup>/g at 28 % conversion and decreased to 5.3 m<sup>2</sup>/g and 5.7 m<sup>2</sup>/g with increase in conversion of 43 % and 85 %. The reduction of grafting density at higher conversion is due to the steric hindrance of growing polymer chain due to the limited surface area.

The effect of method of functionalization was studied using NRHA and NCRHA silica samples. The NRHA samples were synthesized from MRHA silica synthesized via co-condensation, whereas the NCRHA samples synthesized from MCRHA samples synthesized via post modification. The nitrene grafting density observed for silica were 215 μmol/g for NRHA silica, 44 μmol/g for NCPS silica, and 58 μmol/g for NCRHA silica. The co-condensed silica samples NRHA were observed to have higher nitrene loading compared to the NCPS and NCRHA silica samples synthesized via post-modification. The higher nitrene modification of co-condensed silica samples is possibly due to the availability and accessibility of mercaptopropyl group on the surface of silica during thiol-ene reaction. The increase in nitrene functionality increased the polymer grafting of 9.1 μmol/g, which can be observed for PSRHA silica samples at 68 % conversion. Comparatively higher grafting density has been observed at higher conversions for co-condensed NRHA compared to the post-modified NCRHA samples. The surface area and method of functionalization does not influence the polymer grafting studies carried out via 1,3 dipolar cycloaddition of macromonomer possibly due to the limited concentration and lower molecular weight of polymer chains.

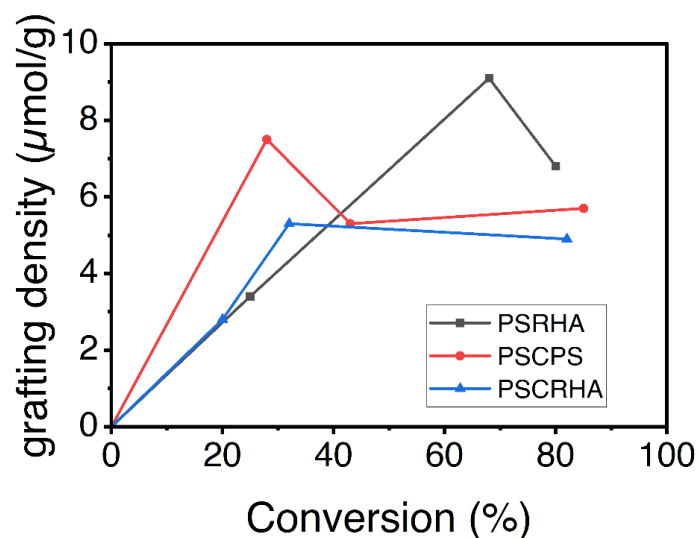


Figure S23. Grafting density determined with respect to conversion for PSRHA, PSCPS and PSCRHA synthesized via ESCP.

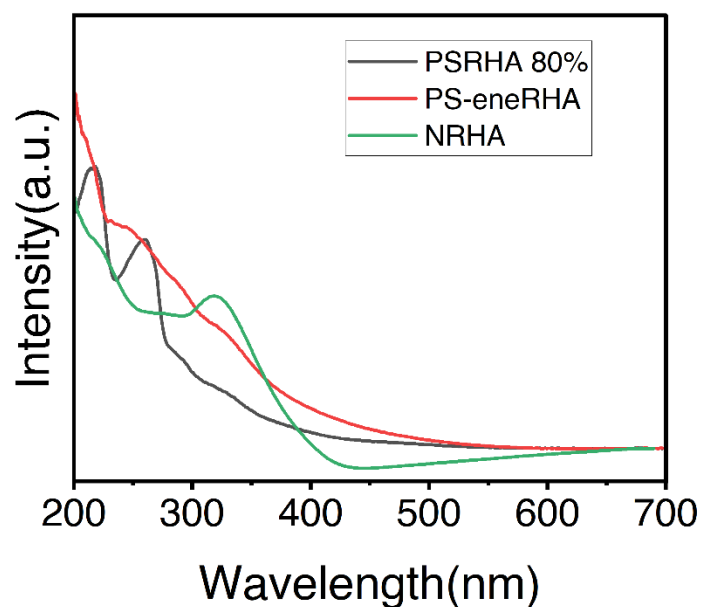


Figure S24. Solid-state UV-visible spectra for nitrene functionalized RHA silica (NRHA), the polystyrene grafted RHA silica via ESCP at 80 % of conversion (PSRHA-80%), and polystyrene grafted RHA silica via 1,3-dipolar cycloaddition of polystyrene macromonomer (PS-eneRHA). The intensity of the band corresponding to nitrene functionality was observed to be decreasing with polystyrene grafting.

## References

- 1 M. Heinenberg and H. Ritter, *Macromol. Chem. Phys.*, 1999, **200**, 1792–1805.
- 2 J. Warneke, Z. Wang, M. Zeller, D. Leibfritz, M. Plaumann and V. A. Azov, *Tetrahedron*, 2014, **70**, 6515–6521.
- 3 *Organic Syntheses, Coll. Vol. 1, p.445 (1941); Vol. 4, p.57 (1925).*, .
- 4 J. F. Lutz and K. Matyjaszewski, *J. Polym. Sci. Part A Polym. Chem.*, 2005, **43**, 897–910.
- 5 O. Altintas, T. Josse, J. De Winter, N. M. Matsumoto, P. Gerbaux, M. Wilhelm and C. Barner-Kowollik, *Polym. Chem.*, 2015, **6**, 6931–6935.